Available online at www.sciencedirect.com
ScienceDirect
Solid State Ionics 177 (2006) 3223–3231
SOLID STATE IONICS
www.elsevier.com/locate/ssi

^{1}H NMR study of proton dynamics in $(NH_4)_3H(SO_4)_2$

Koh-ichi Suzuki [1], Shigenobu Hayashi *

Research Institute of Instrumentation Frontier, National Institute of Advanced Industrial Science and Technology (AIST), Tsukuba Central 5, 1-1-1 Higashi, Tsukuba, Ibaraki 305-8565, Japan

Received 17 May 2006; received in revised form 16 August 2006; accepted 11 September 2006

Abstract

Proton dynamics in $(NH_4)_3H(SO_4)_2$ has been studied by means of ^{1}H solid-state NMR. The ^{1}H magic-angle-spinning (MAS) NMR spectra were traced at room temperature (RT) and at Larmor frequency of 400.13 MHz. ^{1}H static NMR spectra were measured at 200.13 MHz in the range of 135–490 K. ^{1}H spin-lattice relaxation times, T_1, were measured at 200.13 and 19.65 MHz in the ranges of 135–490 and 153–456 K, respectively. The ^{1}H chemical shift for the acidic proton (14.7 ppm) indicates strong hydrogen bonds. In phase III, NH_4^+ reorientation takes place; one type of NH_4^+ ions reorients with an activation energy (E_a) of 14 kJ mol^{-1} and the inverse of a frequency factor (τ_0) of 0.85×10^{-14} s. In phase II, a very fast local and anisotropic motion of the acidic protons takes place. NH_4^+ ions start to diffuse translationally, and no proton exchange is observed between NH_4^+ ions and the acidic protons. In phase I, both NH_4^+ ions and the acidic protons diffuse translationally. The acidic protons diffuse with parameters of E_a=27 kJ mol^{-1} and $\tau_0=4.2\times10^{-13}$ s. The translational diffusion of the acidic protons is responsible for the macroscopic proton conductivity, as the NH_4^+ translational diffusion is slow and proton exchange between NH_4^+ ions and the acidic protons is negligible.

Keywords: Proton dynamics; Proton conduction; Inorganic solid acid; Nuclear magnetic resonance; NMR; Spin-lattice relaxation

1. Introduction

Fuel cells are attractive for electrical power generation because of their high efficiencies and low pollution levels. Polymer electrolyte membrane fuel cells are suitable for transportation systems and mobile uses. As the polymer electrolyte membranes require humid atmospheres, the operating temperature is limited to lower than 373 K. Haile et al. pointed out the advantage of inorganic solid acid salts as fuel cell electrolytes due to circumvent the above limits [1,2]. They demonstrated that water-soluble inorganic solid acid salts such as $CsHSO_4$ and CsH_2PO_4 are used successfully in H_2/O_2 and direct methanol fuel cells, although several improvements are necessary before their practical uses.

It is well known that a high proton conductivity is observed in a high-temperature phase, so-called "a superprotonic phase", of solid acid salts such as $MHXO_4$ and $M_3H(XO_4)_2$ (M=Cs, NH_4, Rb; X=S, Se) families [3–6]. In these compounds, tetrahedral XO_4 anions form hydrogen bond networks. Previously, we studied proton dynamics in $CsHSO_4$ [7–9], $Cs_2(HSO_4)(H_2PO_4)$ [10] and $Rb_3H(SO_4)_2$ [11] by means of ^{1}H solid-state NMR, which is suitable to study the dynamics at atomic levels. We concluded that a motion breaking the hydrogen bonds is rate-determining in the proton diffusion and that the transfer of a proton from a tetrahedron to a neighboring one along a hydrogen bond is faster than the above motion. The microscopic motion well explained the macroscopic electric conductivity.

Triammonium hydrogen disulfate $(NH_4)_3H(SO_4)_2$ belongs to the $M_3H(XO_4)_2$ family, similarly to $Rb_3H(SO_4)_2$ that we previously studied. Crystals of $(NH_4)_3H(SO_4)_2$ undergo phase transitions at 413, 265, 141, 133 and 63 K [12]. The respective phases are denoted as I, II, III, IV, V and VII with decreasing temperature. Phase I is a superprotonic phase, showing a conductivity of about 10^{-2} S cm^{-1} in the (001) plane [13]. The

* Corresponding author. Tel./fax: +81 29 861 4515.
E-mail address: hayashi.s@aist.go.jp (S. Hayashi).
[1] Present address: R&D Division, Energy Business Group, Core Component Business Unit, Sony Corporation, 1-1 Takakura Aza Shimosugishita, Hiwada-machi, Koriyama-shi, Fukushima 963-0531, Japan.

0167-2738/$ - see front matter © 2006 Elsevier B.V. All rights reserved.
doi:10.1016/j.ssi.2006.09.006

crystal structures of phases I and II are well known [14–16], although those of other phases remain unestablished due to ambiguous positions of hydrogen atoms. The structure of phase II is characterized by a zero-dimensional network of hydrogen bonds, which connects two sulfate anions to form an isolated dimer, $[SO_4\text{-}H\cdots SO_4]^{3-}$. On the other hand, a dynamically disordered hydrogen bond network is formed in the (001) plane for phase I. The situation becomes more complex because the NH_4^+ cations participate in numerous additional hydrogen bonds [17]. As described above, ^{1}H solid-state NMR is suitable to study proton dynamics at atomic levels. ^{1}H magic-angle-spinning (MAS) NMR study distinguished the dynamics of acidic protons and ammonium groups for phases II and I [18]. However, the results were rather qualitative. Thus, proton dynamics in $(NH_4)_3H(SO_4)_2$ has not been clarified experimentally in the high-temperature range.

In the present work, we have studied proton dynamics in $(NH_4)_3H(SO_4)_2$ by means of ^{1}H solid-state NMR, especially for the high-temperature phases. We have measured and analyzed ^{1}H MAS NMR spectra, NMR spectra for static samples (static NMR spectra) and spin-lattice relaxation times. We discuss the proton dynamics as quantitatively as possible.

2. Experimental

2.1. Materials

$(NH_4)_3H(SO_4)_2$ crystals were grown by slow evaporation of the aqueous solution containing $(NH_4)_2SO_4$ and a small excess of H_2SO_4, both purchased from Junsei Chemical (Tokyo). The crystalline powder obtained was dried *in vacuo* and then sealed in glass tubes with helium gas for measurements of static NMR spectra and spin-lattice relaxation times (T_1).

2.2. X-ray powder diffraction and thermal analyses

The X-ray powder diffraction pattern was measured by a Rigaku MiniFlex diffractometer with Cu Kα radiation at room temperature. The thermogravimetric and differential thermal analyses (TG–DTA) were performed by a Rigaku Thermo Plus TG 8120 under N_2 flow. The temperature was increased at a rate of 5 K min^{-1} from room temperature to 573 K. The differential scanning calorimetry (DSC) was measured with Rigaku Thermo Plus DSC 8230 in a static N_2 atmosphere. The sample temperature was changed in the range of 153–523 K at heating and cooling rates of 5 K min^{-1}.

2.3. NMR measurements

The ^{1}H MAS NMR spectra were traced at room temperature using a Bruker ASX400 spectrometer at 400.13 MHz. A Bruker MAS probehead with a 2.5-mm zirconia rotor was used. The ordinary single pulse sequence was used with a π/4 pulse and a recycle delay of 30 s. The frequency scale of the spectrum was expressed with respect to neat tetramethylsilane (TMS) by adjusting the signal of adamantane spinning at 8.0 kHz to 1.87 ppm [9,10].

The ^{1}H static NMR spectra were measured with a Bruker ASX200 spectrometer at Larmor frequency of 200.13 MHz in the range of 135–490 K. A Bruker probehead with a solenoid coil was used. The solid echo pulse sequence ($90°_x$-τ_1-$90°_y$-τ_2-echo) was used to trace the spectra and the latter half of the echo signal was Fourier-transformed. The τ_1 and τ_2 values were set at 8.0 μs. The frequency scale of the spectra is expressed with respect to neat TMS by adjusting the signal of pure H_2O to 4.877 ppm [19].

The ^{1}H spin-lattice relaxation times, T_1, were measured with a Bruker ASX200 spectrometer at 200.13 MHz in the range of 135–490 K. The pulse sequences used were the inversion recovery and the progressive saturation recovery followed by the solid echo pulse sequence, which were $180°$-τ-$90°_x$-τ_1-$90°_y$-τ_2-echo and $(90°\text{-}\tau_3)_n$-τ-$90°_x$-τ_1-$90°_y$-τ_2-echo, respectively. The values of τ_1, τ_2 and τ_3 were 8.0, 8.0 and 30 μs, respectively, and τ denoted the variable delay time. The T_1 values were also measured by a Bruker Minispec mq20 spectrometer at 19.65 MHz in the range of 153–456 K to clarify the frequency dependence of T_1. The inversion recovery ($180°$-τ-$90°$) and the saturation recovery ($90°$-τ-$90°$) pulse sequences were used, where τ denoted the variable delay time.

3. Results and discussion

3.1. X-ray powder diffraction and thermal analysis

The X-ray powder diffraction pattern observed at room temperature agrees well with literature data [16]. Thus, we confirm that the sample is phase II of $(NH_4)_3H(SO_4)_2$.

The DSC results show two endothermic thermal anomalies at 265 K (−0.5 kJ mol^{-1}) and 410 K (−3.5 kJ mol^{-1}) and two exothermic ones at 409 K (3.6 kJ mol^{-1}) and 267 K (0.6 kJ mol^{-1}) with increasing and decreasing temperature, respectively, as shown in Fig. 1. These results agree well with literature data [12]. No remarkable thermal hysteresis is observed in $(NH_4)_3H(SO_4)_2$, which is distinct from $Rb_3H(SO_4)_2$ showing a hysteresis of about 50 K [11]. A melting peak is observed at 503 K (−28.8 kJ mol^{-1}). The TG–TDA results in Fig. 2 show

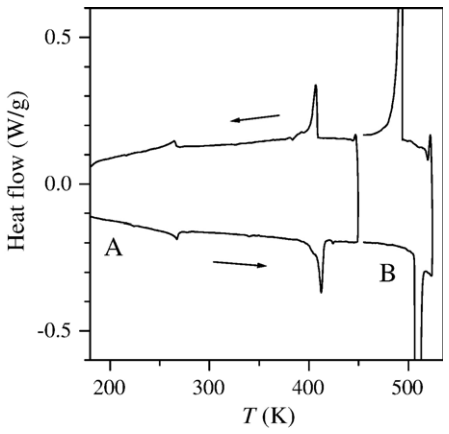

Fig. 1. DSC curves. The sample was heated up to (A) 450 K and (B) 523 K. The arrows indicate the direction of temperature change. Negative heat flow is endothermic.